MOTION AND DEFORMATION ESTIMATION OF CARDIAC ULTRASOUND SEQUENCES USING AN ANATOMICAL B-SPLINE TRANSFORMATION MODEL

B. Heyde[1]*, P. Claus*[1]*, R. Jasaityte*[1]*, D. Barbosa*[1]*,*
S. Bouchez[2]*, M. Vandenheuvel*[2]*, P. Wouters*[2]*, F. Maes*[3]*, J. D'hooge*[1,4]

[1]Cardiovascular Imaging and Dynamics, Catholic University of Leuven, Leuven, Belgium
[2]Department of Anesthesiology, Ghent University, Ghent, Belgium
[3]Medical Image Computing, Catholic University of Leuven, Leuven, Belgium
[4]Norwegian Institute for Science & Technology, Trondheim, Norway

ABSTRACT

We present a novel method for tracking myocardial motion in 2D ultrasound sequences based on non-rigid registration using an anatomical free-form deformation (AFFD) model where the basis functions are locally oriented along the radial and circumferential direction of the left ventricle (LV). This formulation allows us to model the LV motion more naturally compared to previously proposed FFD's defined on a regular Cartesian grid (CFFD). In this paper we compare the performance of the AFFD against the CFFD model in an in-vivo setting. Short-axis images were acquired in five open-chest sheep using sonomicrometry as ground-truth deformation estimates. We demonstrated that regional end-systolic strain values assessed with the AFFD model are comparable with CFFD, while also displaying a statistically lower drift at the end of the cardiac cycle and a better agreement with a manual end-systolic reference. Furthermore, tracking using AFFD was visually more appealing to clinical experts.

Index Terms— Non-rigid registration, anatomical deformation model, strain, echocardiography, in-vivo

1. INTRODUCTION

It is well-known that many cardiac diseases such as coronary artery disease, result in abnormal local wall motion and deformation changes. Various automated methods have been developed to objectively assess regional cardiac deformation using echocardiography.

A popular family of approaches use optical flow methods to estimate myocardial strain. More specifically, block-matching techniques applied on B-mode data, often termed speckle tracking methods [1], have received wide-spread attention in the ultrasound (US) society. This technique is based on the assumption of a stable local speckle pattern between frames to extract local tissue motion from the displacement of intensity patterns. This in turns allows them to accurately capture small regional motion, although a posteriori regularization is typically required as these motion estimates are performed independently from each other. Due to inter-frame speckle decorrelation, this technique may be unreliable when large motions occur or when the image quality is not optimal.

A second group of methods which may be more robust in those cases, use image registration techniques. Free-form deformation (FFD) models where the cardiac deformation field is parametrized using smooth basis functions have been an attractive approach [2]. The global deformation field is estimated simultaneously and regularization is intrinsically embedded in the optimization process (due to the smooth basis functions or the addition of regularization terms in the global cost function). Traditionally, this FFD model has been formulated in Cartesian space (CFFD, see figure 1a) and has already been shown to be successful for US cardiac motion estimation both on scan-converted data (e.g. [3] [4]) and non-scan-converted data (e.g. [5] [6]). For the analysis of MR images, other transformation models more closely matching the LV shape have been proposed (figure 1b), either by using a cylindrical FFD (e.g. [7] [8]) or a prolate spheroidal FFD (e.g. [9]).

In this paper, we propose an anatomical free-form deformation model (AFFD, see figure 1c). In this model, the B-spline basis functions are locally oriented in the radial and circumferential direction of the endocardium. This arrangement naturally enforces smoothness in the physiologically relevant directions. In contrast, CFFD models enforce smoothness in the x and y directions only, which do not relate to the LV anatomy nor correspond to the principal motion directions. Moreover, since the CFFD grid covers the LV cavity completely, it incorrectly treats the blood pool and the myocardium in a similar way whereas the AFFD grid allows for imposing more selective conditions. We first discuss the implementation of the CFFD and AFFD model and then compare the performance of both methods in an in-vivo setting.

2. METHODS

2.1. Cartesian registration

We modeled the inter-frame myocardial displacement with a two-dimensional third-order B-spline tensor-product [2]. Since image intensities at corresponding points between two consecutive frames are similar for intra-modality registration, the sum-of-squared differences was used as an image similarity metric. The optimal displacement field was estimated iteratively with a limited memory Broyden Fletcher Goldfarb Shannon optimization routine with simple bounds (LBFGSB) as this optimizer was found to give a good performance for optimization of a large amount of parameters while also eliminating the need for storing the inverse of the Hessian during the optimization routine. In order to capture small deformations, model complexity was gradually increased in three stages by refining the B-spline grid with a factor of two in every stage. Regularization was performed during the optimization process by the addition of a

The present work was in part funded by the Research Foundation - Flanders (FWO-Vlaanderen, Belgium) under grant G.0693.09. The authors would also like to thank J. Vandenweghe and F. Ingelberts from GE Belgium for providing the ultrasound system.

Corresponding author's email: brecht.heyde@med.kuleuven.be

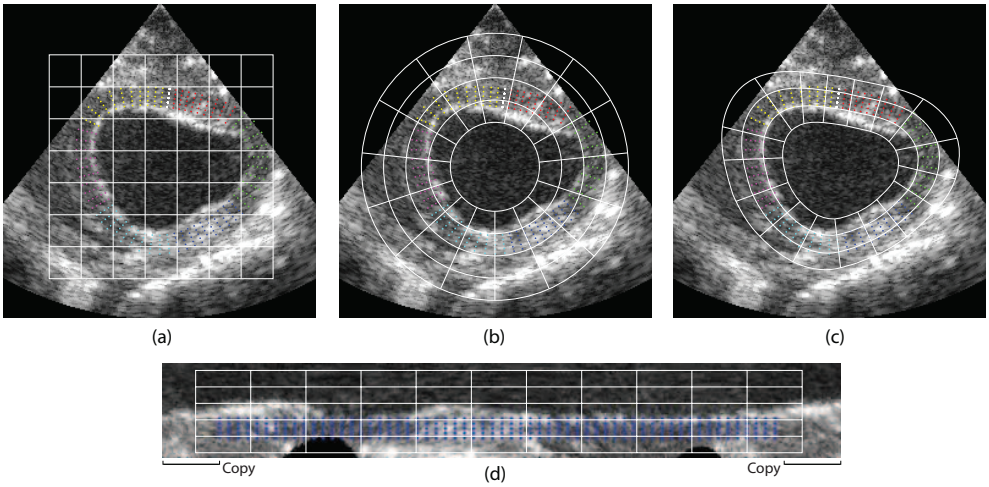


Fig. 1. Schematic overview of different B-spline grids used in image registration: (a) Cartesian grid, (b) Polar grid (equal to 3D slice of cylindrical and prolate spheroidal grid) and (c) proposed anatomical grid. The underlying dots represent a sampled ROI. (d) Resampled image according to the local anatomical coordinate system of (c) together with the transformed ROI.

smoothness penalty (based on the bending energy of a 2D thin sheet of metal), resulting in a spatially smooth displacement field. The method was implemented within the framework of ITK, a collection of open-source C++ image analysis libraries. In every frame, pixels outside the ultrasound sector scan were masked to assure this part of the image did not contribute to the calculations in the registration process. Subsequent images in the cardiac cycle were then registered to each other in a pair-wise fashion.

In order to assess strain within a certain region-of-interest (ROI), the endocardium was first manually contoured in the end-diastolic (ED) frame using custom-made software (Speqle3D). A ROI was then created by expanding the endocardial contour along its normal to represent the myocardium. This region was subsequently populated in the radial and circumferential direction with 5 and 60 sample points respectively, and given a label corresponding to one of the 6 equally spaced segments around the circumference. Using the obtained inter-frame displacement field from the registration results, the cumulative displacement could be calculated in every sample point. Strain $\epsilon_N(t)$ in every point along a certain direction N was then calculated according to:

$$\epsilon_N(t) = \frac{D_N(t) - D_N(0)}{D_N(0)} \quad (1)$$

where $D_N(t)$ is the distance between two adjacent sample points in either the radial or circumferential direction at time point t, and similarly $D_N(0)$ being the respective initial distances (at ED). The estimated strain curves were drift compensated to obtain values of zero strain at ED by distributing the remaining strain offset uniformly over the cardiac cycle. Finally, strain values were averaged within each segment and end-systolic (ES) strain values were extracted in the infero-lateral (IL) wall.

2.2. Anatomical registration

The AFFD grid is locally organized according to the shape of the endocardium (figure 1c). An alternative implementation for an anatomical organized grid is to transform the images to 'anatomical' coordinates first, such that the overlying grid is Cartesian and the endocardium becomes horizontal in the transformed image (figure 1d). In practice, the endocardium is first manually contoured at ED as described in section 2.1. The image is then resampled along the normals of this contour in 50 points. The normals extend both inward towards the blood pool and outward towards the epicardium to ensure that the full myocardium remains inside the transformed image during the whole cardiac cycle. In total, 360 normals are used for the transformation, one for each degree of an imaginary polar grid with the origin being the center of the endocardium. To assure circumferential spatial continuity of the deformation field, a small part of the transformed image is copied on either side (figure 1d). All images in the recorded image sequence, together with the ROI at ED, are transformed to the anatomical space prior to registration.

After frame-to-frame registration, the transformed ROI is propagated in the resampled image sequence and transformed back to Cartesian coordinates. Strain is then calculated according to (1).

3. VALIDATION

To validate the proposed anatomical registration and to compare its performance against conventional cartesian registration, myocardial deformation was estimated with both methods in an in-vivo setting.

3.1. Animal preparation

Five Suffolk sheep (39 ± 5 kg) were anesthetized with a continuous infusion of sufentanil and mechanically ventilated with sevoflurane to maintain normocapnia and normoxia during the intervention. A sternotomy was then performed, and the heart suspended in the pericardial cradle to maintain a normal anatomic configuration. A sonomicrometry system (Sonometrics, London, Ontario, Canada) was used to obtain reference left ventricular deformation measurements. Four ultrasonic microcrystals were placed in a tetrahedral configuration on the myocardium in the mid-IL wall. Three crystals were sutured to the epicardium, resulting in two crystal pairs providing circumferential (ϵ_{CC}) and longitudinal (ϵ_{LL}) reference strain measurements, while a fourth crystal was placed subendocardially just radially to the center crystal to obtain radial strain traces (ϵ_{RR}).

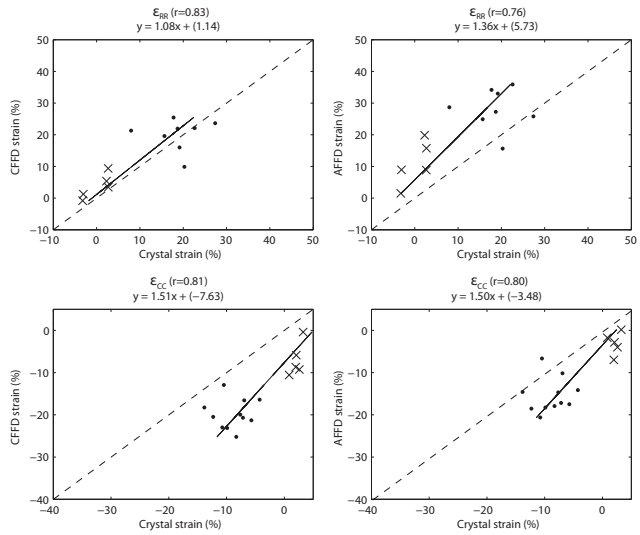


Fig. 2. Scatter plots of estimated ϵ_{RR} (top) and ϵ_{CC} (bottom) for (a) cartesian registration (CFFD) and (b) anatomical registration (AFFD) against reference crystal strain. The dotted line is the line of unity. Points marked with $\times$ indicate ischemic datasets.

3.2. Data acquisition

A GE Vivid7 ultrasound scanner (GE Vingmed, Horten, Norway) equipped with a 2.5 MHz transducer (M4S) was used to acquire short-axis (SAX) B-mode data (frame rate 50-70 Hz). The images were recorded in a plane just parallel to the crystals in order to avoid the crystals showing up as bright spots in the ultrasound data. A liver was used as a stand-off.

Image data and reference crystal measuremens were collected both at rest and during acute ischemia induced by ligating a distal branch of the circumflex coronary artery. In three animals, the range of strain values was also moderated by reducing the inotropic state by esmolol infusion and subsequently increasing it by dobutamine administration. Three radial traces were excluded due to poor quality resulting in 16 and 13 data sets for analysis of ϵ_{CC} and ϵ_{RR} respectively.

3.3. Data analysis

All acquired SAX images were processed according to the two methods as outlined in section 2.1 and 2.2. Care was taken to ensure that parameters of the registration were chosen as similarly as possible for both methods, e.g. same similarity measure (SSD and smoothness penalty), same optimizer (LBFGSB), same B-spline order, same amount of model refinement stages, comparable amount of B-spline grid point covering the myocardium in the final refinement stage and same strain calculation.

In order to obtain reference strain curves, the recorded crystal traces were further post-processed in custom-made software. Reference strain values were also calculated according to equation 1.

3.4. Evaluation criteria

Different criteria were used to evaluate the tracking performance of both registration methods.

- At ES in one region: the obtained systolic strain values for both methods were correlated with the reference strain values obtained by sonomicrometry using the Pearson correlation coefficient and performing a Bland-Altman analysis. Fishers z-transformation was used to compare the strengths of different correlations whereas the bias between the Bland-Altman plots was compared with a paired t-test. P-values lower or equal to 0.05 were considered significant.

- At ES taking all regions into account: by calculating the mean distance d_{ES} and the dice coefficient dc_{ES} between the tracked endocardial contour with a manual reference. For each dataset, the difference between both methods is calculated. A pairwise t-test between these differences was then used to assess whether the performance of one method was significantly different.

- At the end of the cardiac cycle (ED2): by calculating the drift δ_{ED2} as the mean distance of a contour between ED and ED2. This was performed for both the endocardial and the epicardial contour. Performance differences are assessed as described above.

- Qualitative clinical validation: a trained cardiologist was asked to compare the two registration methods both on a global and a segmental level: either AFFD visually tracked better, CFFD visually tracked better or no tracking method was preferred over the other. The image data was randomized and blinded for this observer.

	Bias(%)		LOA	
	ϵ_{RR}	ϵ_{CC}	ϵ_{RR}	ϵ_{CC}
AFFD	9.93	-6.20	[-4.43 24.30]	[-14.39 1.99]
CFFD	2.12	-10.38	[-9.45 13.68]	[-18.47 -2.30]

Table 1. Bland-Altman bias and limits of agreement (LOA).

	Global	Segmental					
		I	IS	AS	A	AL	IL
AFFD	44	0	19	44	37	13	19
CFFD	31	13	13	19	19	13	19
Equal	25	87	68	37	44	74	62

Table 2. Preference for either method (AFFD,CFFD) or no preference (Equal) in percentage of cases, based on tracking performance as judged by a trained cardiologist on a global and segmental level. AFFD/CFFD = anatomical/cartesian FFD. Segmental codes: A = anterior, AL/IL = antero/inferolateral, I = inferior, IS/AS = infero/anteroseptal.

4. RESULTS

The correlation between the estimated ES strain and the reference ES strain values in the radial direction was r=0.83 and r=0.76 for CFFD and AFFD respectively, and respectively r=0.81 and r=0.80 in the circumferential direction (figure 2, $p<0.01$ everywhere). No significant differences between ϵ_{RR} correlations and ϵ_{CC} correlations were found (p=0.69 and p=0.91 respectively). Results for Bland-Altman analysis are summarized in table 1. Figure 3 shows d_{ES} of the endocardial contour (panel a) and δ_{ED2} of the endocardial (panel b) and epicardial contour (panel c). The dc_{ES} of the endocardial contour (not shown here) was higher for the AFFD method (0.012) but this difference was not significant (p=0.09). Finally, the tracking performance as interpreted by the cardiologist is presented in table 2.

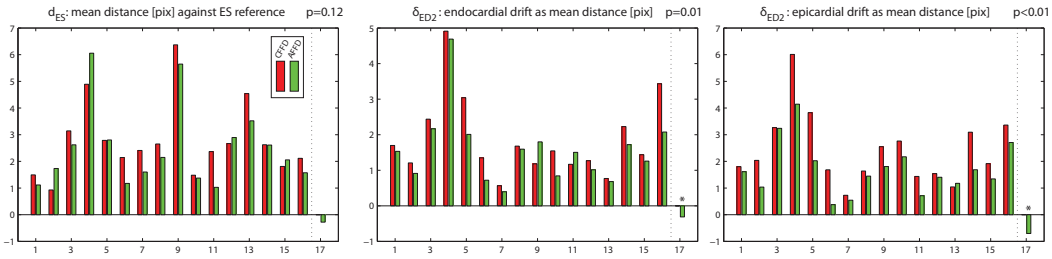


Fig. 3. Performance of CFFD (red) against AFFD (green) for the 16 datasets. Column 17 shows the mean difference between both methods.

5. DISCUSSION

In this work, both methods showed a good correlation against sonomicrometry in both directions (figure 2). Moreover, the performance of the AFFD model was comparable to the CFFD model for ϵ_{RR} (p=0.69) and ϵ_{CC} (p=0.91). Furthermore, the ϵ_{CC} bias was significantly lower for AFFD (p<0.01) and the limits of agreement (LOA) were also tighter (table 1). However, Bland-Altman analysis of ϵ_{RR} favored the CFFD model. The radial movement might have been influenced too much by the circumferential movement as the bending energy is currently isotropic. In the future it may thus be better to consider an anisotropic bending energy. It is important to note that these measures all describe the tracking performance of only one particular region (containing the crystals) and at only one instance of the cardiac cycle (end-systole). Other criteria were therefore also investigated.

The d_{ES} and dc_{ES} of the endocardial contour both favored the AFFD model, but the differences were not significant (figure 3a, p=0.12). In terms of the endo- and epicardial drift δ_{ED2} (figure 3b-c) the AFFD model performed significantly better (p$\leq$0.01). Furthermore, a clinical expert found the cardiac tracking using AFFD visually equal or more appealing then the CFFD model in all walls apart from the inferior segment (table 2). However the difference between both methods was also the lowest here: 13%. Most datasets where CFFD was preferred over AFFC were ischemic cases. They showed a large asymmetric motion in the septal wall, which caused an overlap of a limited amount of normals towards the blood cavity. Due to the sampling process, physiological septal motions in the anatomical grid were translated in non-physiological folding motions in cartesian space. This however occurred only in a limited region.

The major rationale behind this work is that an AFFD model offers several advantages over the CFFD model. First of all, the organisation of the B-spline grid more closely matches the shape and motion of the heart. CFFD has a shape mismatch which can cause B-spline spans to contain few or no myocardial displacement measurements, and which may cause additional errors. While the performance of both methods is comparable, the AFFD model is able to do so through a more efficient myocardial grid coverage, thus using less parameters and leading to a reduced inter-frame registration time (10.1$\pm$0.6s vs 16.1$\pm$8.4s for the CFFD model). Moreover, since the CFFD grid covers the LV cavity completely, it incorrectly treats the blood pool and the myocardium in a similar way, whereas an AFFD model allows to impose conditions more closely coupled to the LV physiology, e.g. the smoothness penalty is naturally aligned with the fibre and cross-fibre directions in the myocardium. It also allows to include a priori knowledge in a more straight-forward manner, e.g. imposing volume conservation on the myocardium only or adding a segmentation penalty in the cost function. The endocardial delineation is a straight line in the cardiac grid, which simplifies their implementation. The effect of these cost functions on tracking performance remains the topic of future research.

A potential limitation of the present study is that the anatomical B-spline grid is currently fixed, i.e. all the images in the acquired sequence are resampled based on the same initial normals. In the future it might be better to employ a dynamic grid which moves together with the propagated endocardial wall. This should also prevent overlapping of the normals towards the center of the cavity in case large deformations occur.

6. CONCLUSIONS

In this work, we compared the performance of a novel FFD using a B-spline transformation model defined on an anatomical grid, with a traditional Cartesian FFD model. We demonstrated that regional end-systolic strain values assessed with the AFFD model are comparable with the CFFD model, while also displaying a statistically lower drift at the end of the cardiac cycle and a better agreement with a manual end-systolic reference. Furthermore, tracking using AFFD was visually more appealing to clinical experts.

7. REFERENCES

[1] L Bohs and G Trahey, "A novel method for angle independent ultrasonic imaging of blood flow and tissue motion," *IEEE Trans Biomed Eng*, vol. 38, no. 3, pp. 280–286, 1991.

[2] J Kybic and M Unser, "Fast parametric elastic image registration," *IEEE TIP*, vol. 12, no. 11, pp. 1427–1442, 2003.

[3] M Ledesma-Carbayo et al., "Spatio-temporal nonrigid registration for ultrasound cardiac motion estimation," *IEEE TMI*, vol. 24, no. 9, pp. 1113–1126, 2005.

[4] B Heyde et al., "Performance of elastic image registration against speckle tracking for 2D cardiac motion and strain estimation," in *Proc. IEEE Int Ultrasonics Symp*, 2011, In press.

[5] A Elen et al., "Estimation of 3D cardiac deformation using spatio-temporal elastic registration of non-scanconverted US data," in *SPIE Med Imaging*, 2008, vol. 6920, pp. 69200R1–9.

[6] A Myronenko et al., "Maximum likelihood motion estimation in 3D echocardiography through non-rigid registration in spherical coordinates," in *FIMH*, 2009, vol. 5528 of LNCS, pp. 427–436.

[7] R Chandrashekara et al., "Analysis of myocardial motion and strain patterns using a cylindrical B-spline transformation model," in *IS4TM*, 2003, vol. 2673 of LCNS, pp. 88–99.

[8] X Deng and T Denney, "Three-dimensional myocardial strain reconstruction from tagged MRI using a cylindrical B-spline model," *IEEE TMI*, vol. 23, no. 7, pp. 861–867, 2004.

[9] J Li and T Denney, "Left ventricular motion reconstruction with a prolate spheroidal B-spline model," *Phys Med Biol*, vol. 51, no. 3, pp. 517–537, 2006.